

Exchange - correlation effects in semiconductor double-quantum-wire systems

To cite this article: N Mutluay and B Tanatar 1997 *J. Phys.: Condens. Matter* **9** 3033

View the [article online](#) for updates and enhancements.

Related content

- [Collective excitations and instabilities in double-wire electron - hole systems](#)
N Mutluay and B Tanatar
- [Coupled charged Bose quantum wires](#)
R K Moudgil, K Tankeshwar, K N Pathak et al.
- [Electron correlations in an electron bilayer at finite temperature: Landau damping of the acoustic plasmon](#)
D S Kainth, D Richards, H P Hughes et al.

Recent citations

- [Mass-asymmetry effects in coupled electron-hole quantum wire system](#)
R. K. Moudgil *et al*
- [Quantum confinement in mesoscopic annular regions with \$C_{2v}\$ and \$C_{3v}\$ symmetries](#)
Achint Kapoor *et al*
- [Plasmons and magnetoplasmons in semiconductor heterostructures](#)
Manvir S. Kushwaha



IOP | ebooks™

Bringing you innovative digital publishing with leading voices to create your essential collection of books in STEM research.

Start exploring the collection - download the first chapter of every title for free.

Exchange–correlation effects in semiconductor double-quantum-wire systems

N Mutluay and B Tanatar

Department of Physics, Bilkent University, Bilkent, 06533 Ankara, Turkey

Received 15 October 1996, in final form 18 December 1996

Abstract. We study the short-range correlations in a double-quantum-wire structure within the self-consistent scheme of Singwi, Tosi, Land, and Sjölander. The local-field factors and static correlation functions are calculated for electron and electron–hole double-wire systems. The ground-state energy and collective excitations are discussed. It is found that the interwire correlations become quite important for electron–hole systems. Comparisons with the random-phase approximation and Hubbard approximation are made for various calculated quantities.

1. Introduction

The recent progress in fabrication techniques such as molecular beam epitaxy and lithographic methods has made it possible to study quasi-one-dimensional (Q1D) electron systems, which occur in semiconducting structures, in which the electrons are confined to move freely only in one space dimension. Experimental and theoretical work continues to be a subject of interest, the main motivation coming from their technological potential such as in high-speed electronic devices and quantum-wire laser applications. Other than the practical implications, electrons in Q1D structures provide an interesting many-body system as regards condensed-matter theories. In this paper we study the ground-state correlations of a double-quantum-wire system at zero temperature. Such structures, analogous to the double-quantum-well systems recently studied, are important in our understanding of the correlation effects in low-dimensional systems.

Collective excitations in quantum-wire systems were experimentally studied by spectroscopic methods [1, 2]. Various theoretical aspects of Q1D structures have been investigated in connection with GaAs-based materials [3–8]. The remarkable success of the random-phase approximation (RPA) in interpreting the excitation spectra of quantum wires is attributed [4, 9] to the limited phase space of Q1D systems. The applicability of the Fermi-liquid approach (as opposed to the Tomonaga–Luttinger-type picture [10]) to the semiconducting quantum-wire systems has been discussed in detail [11] with the result that finite-temperature and disorder effects allow the formation of a well-defined Fermi ‘surface’ in such systems. These predictions are in very good agreement with the experimental observation [1, 2] of collective excitations in GaAs quantum wires. The ground-state correlation effects in single quantum wires were explored [12–14] going beyond the random-phase approximation (RPA). To include corrections due to exchange–correlation effects associated with the charge fluctuations, the method of Singwi, Tosi, Land, and Sjölander (STLS) [15] offers a physically motivated improvement over the RPA. Density-functional and self-consistent methods have also been employed in various calculations [16, 17].

Our chief aim in this paper is to develop the self-consistent scheme of Singwi *et al* [15] to calculate exchange–correlation effects in double-quantum-wire systems. We specialize to equal-density electron and electron–hole (one wire has electrons as charge carriers whereas the other has holes) systems to study the effects of intra- and interwire correlations. The presence of additional charges in the second quantum wire enhances the correlation effects compared with the case of a single wire. Intra- and interwire correlations are quite different in nature because the charge carriers can only move in their respective wires (in the absence of tunnelling) and exchange interactions become important. Interwire correlations increase with decreasing wire separation. The STLS approximation has proved very useful in double-layer two-dimensional electron gas systems [18–20]. The RPA has been found to overestimate the static properties. On the other hand, the STLS approximation is believed to give reliable results if the carrier density is not very low. There is yet another motivation for considering double-wire systems within the STLS approximation. A charge-density-wave (CDW) instability in these systems has been predicted [21, 22] to occur, as in the case of double-quantum-well structures [23]. Being a many-body effect, this instability requires an accurate description of the local-field corrections in its analysis. In this work we concentrate on the fully self-consistent evaluation of the static structure factors and local-field corrections in electron and electron–hole double-wire systems.

The rest of this paper is organized as follows. In section 2 we outline the method of STLS for the density–density response in a double-wire system. Our numerical results for the static structure factors, local-field corrections, ground-state energy, and collective excitations in electron and electron–hole double-wire structures are presented in section 3. We conclude with a brief summary of our results.

2. Theory

We assume that the Q1D electrons in each wire are embedded in a uniform positive background to maintain overall charge neutrality. The density–density response function (matrix) of a double-wire electron (or electron–hole) system in its extension to a multi-component case is given by [18, 24]

$$[\chi(Q)]^{-1} = \begin{bmatrix} [\chi_{11}^0(Q)]^{-1} - V_{11}(q)[1 - G_{11}(q)] & -V_{12}(q)[1 - G_{12}(q)] \\ -V_{21}(q)[1 - G_{21}(q)] & [\chi_{22}^0(Q)]^{-1} - V_{22}(q)[1 - G_{22}(q)] \end{bmatrix} \quad (1)$$

where $\chi_{ii}^0(Q)$ is the zero-temperature 1D free-electron [25] density–density response function for the i th wire (in this equation, Q represents q, ω). We use the particle-number-conserving expression [26]

$$\chi^0(q, \omega; \gamma) = \frac{(\omega + i\gamma)\chi^0(q, \omega + i\gamma)}{\omega + i\gamma[\chi^0(q, \omega + i\gamma)/\chi^0(q, 0)]} \quad (2)$$

to account for the disorder effects through the phenomenological parameter γ , in order to justify the use of the Fermi-liquid approach in Q1D electron systems. The fluctuation-dissipation theorem enables us to express the static structure factors $S_{ij}(q)$ in terms of the response functions:

$$S_{ij}(q) = -\frac{1}{n\pi} \int_0^\infty d\omega \chi_{ij}(q, i\omega) \quad (3)$$

where the frequency integration is to be performed along the imaginary axis to better capture the contribution from collective modes [27]. The handling of the plasmon contribution

becomes important for Q1D systems since the collective modes do not undergo Landau damping, and exist over a large range of q -values. The $G_{ij}(q)$ are the static local-field factors arising from the short-range Coulomb correlations and the exchange–correlation effects for the density–density responses. Setting $G_{ij} = 0$ in the density–density response matrix, one recovers the RPA. The choice of $G_{ij}(q)$ in the approximation scheme of STLS depends on an *ansatz* which decouples the two-particle distribution function into a product of two one-particle distribution functions multiplied by the pair-correlation function. They are given by [12, 14, 15]

$$G_{ij}(q) = -\frac{1}{n} \int_{-\infty}^{\infty} \frac{dk}{2\pi} \frac{kV_{ij}(k)}{qV_{ij}(q)} [S_{ij}(q-k) - \delta_{ij}] \quad (4)$$

where n is the linear electron density assumed to be the same for both wires. In terms of the Fermi wave-vector we have $n = 2k_F/\pi$. The electron gas parameter is defined as $r_s = \pi/(4k_F a_B^*)$, in which $a_B^* = \epsilon_0/(e^2 m^*)$ is the effective Bohr radius in the semiconducting wire with background dielectric constant ϵ_0 and electron effective mass m^* .

The model that we use in our calculation for the Q1D electron system was developed by Gold and Ghazali [6]. It consists of two cylindrical quantum wires of radius R each in an infinite potential well and separated by a distance d ($d > 2R$). We assume that only the lowest subband in each given quantum wire is occupied. The intra- and interwire Coulomb interactions between particles in their lowest subbands within this model are given by [6, 21]

$$V_{11}(q) = \frac{e^2}{2\epsilon_0} \frac{144}{(qR)^2} \left[\frac{1}{10} - \frac{2}{3(qR)^2} + \frac{32}{3(qR)^4} - 64 \frac{I_3(qR)K_3(qR)}{(qR)^4} \right] \quad (5)$$

$$V_{12}(q) = \frac{e^2}{2\epsilon_0} (96)^2 \left[\frac{I_3(qR)}{(qR)^3} \right]^2 K_0(qd) \quad (6)$$

respectively, where $I_n(x)$ and $K_n(x)$ are the modified Bessel functions. Notable features of the Gold and Ghazali [6, 21] model are that the intrawire potential behaves as $\sim |\ln(qR)|$ for long wavelengths and the interwire potential as $\sim |\ln(qd)|$, characteristic of various other models. The quantum-wire model used in a Q1D structure determines the Coulomb interaction potential and some asymptotic properties of the local-field factor as discussed by Fantoni and Tosi [28]. Although the realistic quantum wires are far from being spherical in cross-section, and never have infinite barriers, the present model serves as a convenient example of coupled-wire geometry.

The ground-state energy (per particle) of the double-wire electron system is expressed as the sum of kinetic energy and exchange–correlation energy parts. The kinetic energy contribution is simply $T = \pi^2/(24r_s^2)$ Ryd*, where the ‘effective rydberg’ energy unit is defined as $1 \text{ Ryd}^* = e^2/(2\epsilon_0 a_B^*)$. We use the standard manipulations related to the ground-state-energy theorem of Pauli to express the exchange–correlation energy as

$$E_{xc} = -\frac{1}{8r_s^2} \sum_{ij} \int_0^{r'_s} dr'_s \gamma_{ij}(r'_s) \quad (7)$$

where

$$\gamma_{ij}(r_s) = -\frac{2\epsilon_0}{e^2 k_F} \int_0^{\infty} dq V_{ij} [S_{ij}(q; r_s) - \delta_{ij}] \quad (8)$$

in which the self-consistent values of the static structure factors $S_{ij}(q)$ are used. Extension of the above formalism to a system in which one of the quantum wires has holes for charge carriers requires only straightforward modifications.

3. Results and discussion

We solve the above set of equations (equations (1)–(4)) that describe the structure factors and local-field corrections for the density–density response in a double-wire system (both for the electron and electron–hole cases) self-consistently. The numerical accuracy attained is typically 0.01%. Material parameters appropriate for GaAs-based structures are used so that $m^* = 0.07m_e$ (m_e is the free-electron mass) and $\epsilon_0 = 12.9$. In the electron–hole double wires we take the electron and hole effective mass ratio $m_e^*/m_h^* = 0.134$, which corresponds to $m_h^* = 0.5m_e$. Furthermore, in the case of the coupled electron–hole double-wire system we take a single hole band. The method that we use may be generalized to include valence-band degeneracy effects at the expense of a heavy computational effort. The phenomenological disorder parameter γ that we use in the density–density response function does not influence the converged $S_{ij}(q)$ and $G_{ij}(q)$ significantly for $\gamma \lesssim 0.1E_F$, except that the fluctuation-dissipation integral in equation (3) becomes free of singularity at $q = 2k_F$. As the broadening parameter γ becomes comparable to E_F , noticeable effects on $S_{ij}(q)$ and $G_{ij}(q)$ start to occur. In this work we limit our calculations to the case where $\gamma = 0.01E_F$. We mention that the particle-number-conserving expression that we use has the same form as in more sophisticated approaches, where it is replaced by the wave-vector- and frequency-dependent memory function [29] $\gamma(q, \omega)$. The phenomenological γ may be related to the measured mobilities in quantum wires by the usual relaxation-time expression.

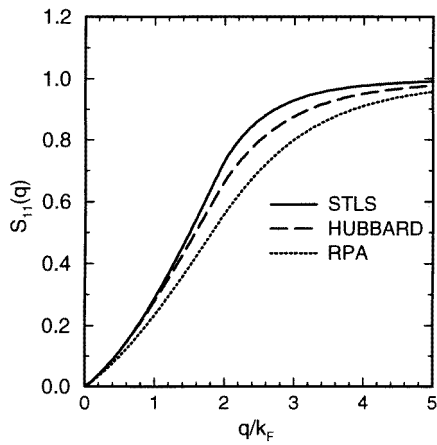


Figure 1. The structure factor $S_{11}(q)$ in a double-wire electron system at $r_s = 2$, $R = 2a_B^*$, and $d = 5a_B^*$, in the STLS (solid), and the Hubbard approximations (dashed), and in the RPA (dotted).

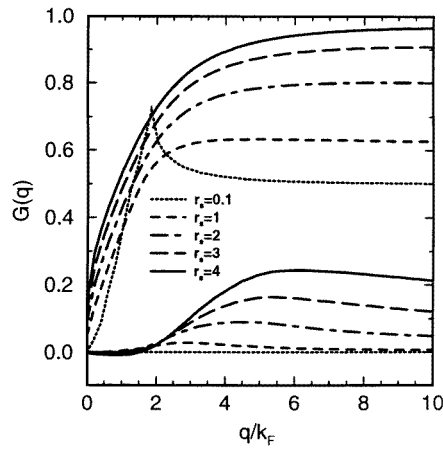


Figure 2. The intrawire and interwire local-field factors $G_{11}(q)$ (upper curves) and $G_{12}(q)$ (lower curves) for a double-wire electron system with $R = 2a_B^*$ and $d = 5a_B^*$. In both cases, the dotted, short-dashed, dot-dashed, long-dashed, and solid lines are for $r_s = 0.1, 1, 2, 3,$ and 4 , respectively.

We first discuss our results for the double-wire electron system. The intrawire static structure factor $S_{11}(q)$, for small r_s , resembles the noninteracting structure factor given by the Hartree–Fock (HF) approximation. As the density is lowered, correlation effects become more important. We compare different approximations to $S_{11}(q)$ in figure 1 for a double-wire electron system at $r_s = 2$. The solid, dashed, and dotted lines show the STLS, and the Hubbard approximations, and the RPA, respectively. The Hubbard approximation (HA) to the local-field factor is obtained from equation (4) by replacing the static structure

factor by the HF expression. This yields approximately

$$G_{ij}(q) = \frac{1}{2} \frac{V_{ii}(\sqrt{q^2 + k_F^2})}{V_{ii}(q)} \delta_{ij}.$$

The Hubbard approximation is a simplified attempt to go beyond the RPA in which the Pauli hole around electrons is taken into account but the correlations are neglected. Note that the $S_{\text{STLS}}(q)$ shown in figure 1 is considerably different from $S_{\text{RPA}}(q)$ and $S_{\text{HA}}(q)$. Similar behaviours of the static structure factor in Q1D systems have been obtained in various other calculations [12–14]. The interwire structure factor $S_{12}(q)$ is about an order of magnitude smaller than $S_{11}(q)$ and negative in the range of q -values of interest.

The intrawire local-field factor $G_{11}(q)$ for different densities is shown in figure 2 (upper curves). As r_s increases, the magnitude of $G_{11}(q)$ approaches unity for large wave-vectors. In the opposite limit, as $r_s \rightarrow 0$, $G_{11}(q)$ exhibits a peak at around $q = 2k_F$. We find that G_{11} is not very sensitive to the value of the wire separation d , as in the case of double-layer systems [19]. Our results for $G_{11}(q)$ are in qualitative agreement with the calculations of Wang and Ruden [22] and single-wire calculations of Friesen and Bergersen [12]. It should be noted that Wang and Ruden [22] set $G_{12}(q) = 0$ from the outset, whereas in our calculations both intra- and interwire components of the local-field factor are determined self-consistently. Although the simplification $G_{12} = 0$ is justified in electron double-wire systems, as we shall see later in the electron–hole systems G_{12} cannot be neglected because of the stronger correlations. The interwire local-field factor $G_{12}(q)$ for different densities is shown in figure 2 (lower curves) where the same double-quantum-wire parameters are used as in the previous cases. It is to a great extent negligible (except at large r_s) compared to G_{11} , and diminishes for large wave-vectors.

The self-consistent local-field corrections and static structure factors for electron–hole

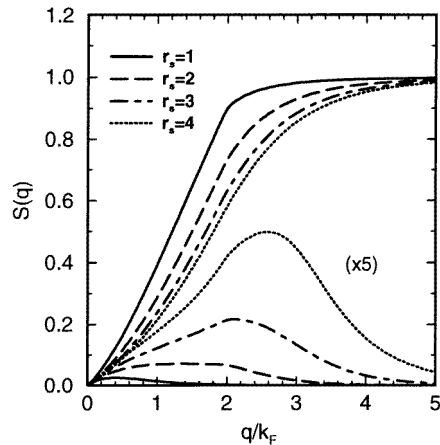


Figure 3. The static structure factors $S_{11}(q)$ and $S_{12}(q)$ (lower curves) in a double-wire electron–hole system for different densities: $r_s = 1$ (solid curve), $r_s = 2$ (dashed curve), $r_s = 3$ (dot-dashed curve), and $r_s = 4$ (dotted curve).

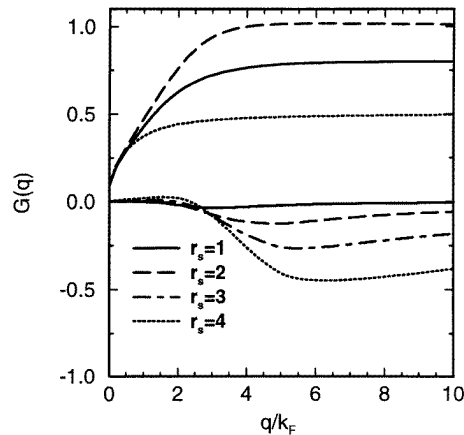


Figure 4. Upper part: the intrawire local-field factors $G_{11}(q)$ (solid curves) and $G_{22}(q)$ (dashed curves) in an electron–hole double-wire system with $R = 2a_B^*$ and $d = 5a_B^*$ at $r_s = 2$. The dotted line represents the Hubbard approximation to $G(q)$. Lower part: the interwire local-field factor $G_{12}(q)$ at different densities: $r_s = 1$ (solid curve), $r_s = 2$ (dashed curve), $r_s = 3$ (dot-dashed curve), and $r_s = 4$ (dotted curve).

double-wire systems are calculated in a similar manner to those of an electron system. The RPA for electron–hole systems is even less reliable because the attractive interwire interaction has a larger effect than the repulsive interaction. The failure of the RPA is revealed in the unphysical pair-correlation functions which are partially remedied in the self-consistent approach [18, 19]. In a multi-component system, the improvements brought about by the STLS scheme over the RPA are the result of taking multiple scatterings between electrons and holes into account (albeit in an approximate way). Even though the carrier densities in two wires are kept the same, the differences in the effective masses for electrons and holes render the noninteracting response functions χ_{11}^0 and χ_{22}^0 different. Consequently, altogether six quantities are determined iteratively. The calculated structure factors $S_{ij}(q)$ again reveal considerable differences between the self-consistent and RPA results. In contrast to the electron double-wire system, the interwire structure factor $S_{12}(q)$ becomes positive. In figure 3 the intra- and interwire static structure factors $S_{11}(q)$ and $S_{12}(q)$ are shown for different densities. The intrawire local-field factors $G_{11}(q)$ and $G_{22}(q)$ for a double-wire electron–hole system at density $r_s = 2$ are depicted in the upper part of figure 4. For comparison we also plot the Hubbard approximation to $G(q)$ (the dotted line). The interwire component $G_{12}(q)$ for various densities is shown in the lower part of figure 4. In an electron–hole double-wire system, $G_{12}(q)$ is predominantly negative.

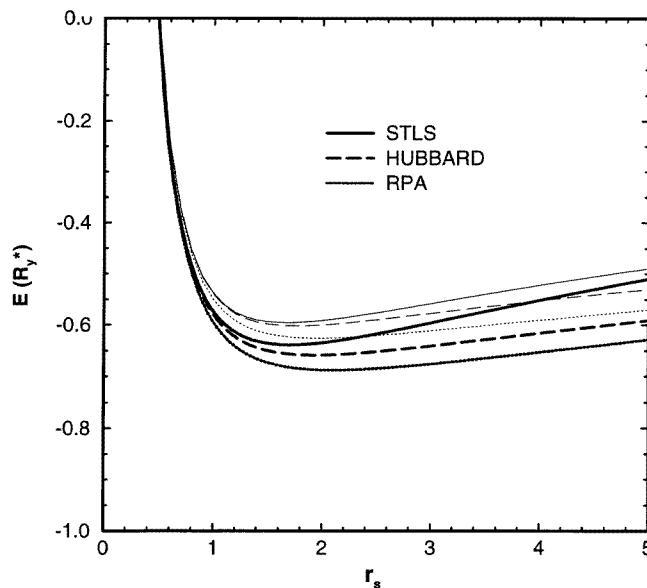


Figure 5. The ground-state energy of a double-wire electron (thin lines) and electron–hole (thick lines) systems as a function of density at a wire separation of $d = 5a_B^*$. The energies in the STLS approximation (solid curve), HA (dotted curve), and RPA (dashed curve) are compared for $R = 2a_B^*$ wires.

The ground-state energy of a double-wire electron system in different approximations is displayed in figure 5 (thin lines). All three curves exhibit minima which lie at around $r_s \approx 1.5$. The RPA yields an overestimate for the ground-state energy because the short-range correlation effects are not incorporated. The Hubbard approximation partially remedies this, but E_{HA} is still below the STLS ground-state energy. Since the interwire interaction decays exponentially (i.e., $\sim e^{-qd}$) for large wave-vectors, the correlation energy

contribution goes to zero as the wire separation d increases. The ground-state energy then becomes the sum of two independent wires. Similar behaviour has also been noted for double-layer electron systems [18, 19]. We find that the ground-state energy does not show a strong dependence on the wire separation for an equal-density system with $R = 2a_B^*$ and $d > 5a_B^*$. This is mainly because of the weak d -dependence of the local-field factor $G_{11}(q)$ discussed above. Nevertheless, for very low densities ($r_s > 5$) it might be possible to have stronger separation distance dependence of the ground-state energies in double-wire systems. More reliable and elaborate approaches would then be required to study this regime. The ground-state energy in an electron–hole double-wire structure is also shown in figure 5 (thick lines). As in the electron double-wire system, the correlation effects are gradually built in with different approximations. We note that the RPA produces a very loosely bound system (as in the electron double-wire case) since the ground-state-energy minimum is less noticeable than those in the other approximations. This once again shows that the effects of correlations are more important in electron–hole double wires than those in electron systems. We observe that departures from the RPA and Hubbard-approximation results become significant for $r_s > 1$. In general, the ground-state energies are slightly lower (in magnitude) for the electron–hole double wires. We have also calculated the separation dependence of the ground-state energy and found no significant dependence for $d > 8a_B^*$ in $R = 2a_B^*$ double-wire systems. For the smallest wire separations (i.e. $d \sim 4a_B^*$) our calculations on electron–electron and electron–hole cases become less reliable, since the tunnelling effects are not included in the formalism that we use. Thus we believe that a more complete theory would address the problem of the separation dependence of the ground-state energy better.

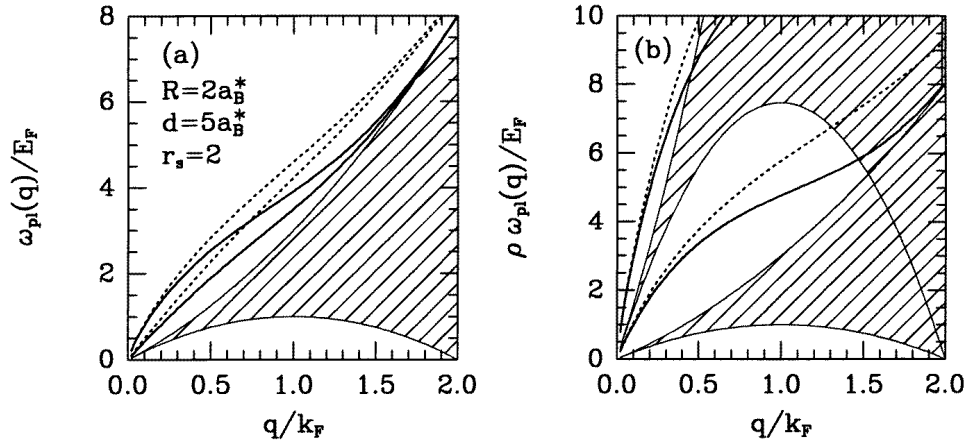


Figure 6. (a) The plasmon dispersions in a double-wire electron system with $R = 2a_B^*$ and $d = 5a_B^*$ at $r_s = 2$. (b) The plasmon dispersions in a double-wire electron–hole system in the long-wavelength approximation at $r_s = 1$. In both cases dashed and solid lines stand for the RPA and STLS approximation results. The shaded regions indicate the single-particle excitation regions.

Collective excitations in a double-wire electron gas when correlation effects are included are obtained from the solution of the screening function

$$\begin{aligned} \varepsilon(q, \omega) = & [1 - V_{11}(q)[1 - G_{11}(q)]\chi_{11}^0(q, \omega)] [1 - V_{22}(q)[1 - G_{22}(q)]\chi_{22}^0(q, \omega)] \\ & - [V_{12}(q)[1 - G_{12}(q)]]^2 \chi_{11}^0(q, \omega)\chi_{22}^0(q, \omega) = 0 \end{aligned} \quad (9)$$

in which we use the disorder-free response functions $\chi_{ii}^0(q, \omega)$. In the case of an equal-density double-wire electron system (with $V_{11} = V_{22}$, $G_{11} = G_{22}$ and $\chi_{11}^0 = \chi_{22}^0$) the plasmon dispersions are given by [4, 23]

$$\omega_{\text{pl}}^2(q) = \frac{\omega_+^2 e^{A_{\pm}(q)} - \omega_-^2}{e^{A_{\pm}(q)} - 1} \quad (10)$$

where $\omega_{\pm} = |q^2/2m^* \pm qk_F/m^*|$ define the boundaries of the single-particle excitation region, and $A_{\pm}(q) = (\pi q/m^*)/[V_{11}(1 - G_{11}) \pm V_{12}(1 - G_{12})]$. The \pm signs refer to in- and out-of-phase oscillations of the charges, and the collective excitations are labelled as the optical and acoustic plasma modes, respectively, according to their long-wavelength behaviour. The long-wavelength limit of the plasmon dispersions (in the RPA) in double-wire electron systems was discussed by Li and Das Sarma [4] and by Gold [8]. We show the effects of exchange and correlation described by the local-field factors on the plasmon dispersion of a double-wire electron system in figure 6(a). The number density in each wire is characterized by $r_s = 2$, and we take $R = 2a_B^*$ and $d = 5a_B^*$. The solid and dotted lines indicate $\omega_{\text{pl}}(q)$ with and without (the RPA) the local-field corrections, respectively. The upper and lower (optical and acoustic) plasmon branches merge together at a finite wave-vector q_c , and approach the upper boundary of the particle-hole boundary much more quickly, since the local fields tend to soften the plasmon dispersions. As the separation d between the wires decreases, the interwire correlation effects become more important and the critical wave-vector q_c decreases.

In the case of electron-hole double quantum wires, the full collective excitations are obtained by solving equation (9) numerically. The long-wavelength limits of the dispersion relations are calculated similarly to the 2D and Q1D, two-component electron liquid cases [30]. The difference here is that electron and hole wires are spatially separated. The optical plasmons exist in the region above the single-particle continuum of electrons. We obtain the optical plasmon mode dispersion in the long-wavelength limit as

$$[\omega_{\text{pl}}^{\text{op}}(q)]^2 = \frac{B}{2} + \left(\frac{B^2}{4} - C \right)^{1/2} \quad (11)$$

where

$$B = \left(\frac{16r_s}{\pi^2} \right) \frac{q^2}{\rho} [F_{11}(1 - G_{11})/\rho + F_{11}(1 - G_{22})]$$

and

$$C = \left(\frac{16r_s}{\pi^2} \right)^2 \frac{q^4}{\rho^3} [F_{11}^2(1 - G_{11})(1 - G_{22}) - F_{12}^2(1 - G_{12})^2].$$

In the above expressions, we measure the plasmon energy in terms of the Fermi energy of the holes ($E_{Fh} = k_F^2/(2m_h^*)$), $\rho = m_e^*/m_h^*$, and we also write $V_{11}(q) = e^2 F_{11}/(2\epsilon_0)$, etc. Since the mass ratio $1/\rho \gg 1$, equation (9) admits another solution (acoustic plasmons) for energies above the single-particle continuum of holes, and below the single-particle continuum of electrons. We calculate the long-wavelength dispersion of acoustic plasmons to be

$$[\omega_{\text{pl}}^{\text{ac}}(q)]^2 = \frac{\omega_+^2 e^{A'/B'} - \omega_-^2}{e^{A'/B'} - 1} \quad (12)$$

where

$$A' = 1 - F_{11}(1 - G_{11}) \left(\frac{2r_s}{\pi^2} \right) \frac{2}{q} \ln \left| \frac{\omega_-}{\omega_+} \right|$$

and

$$B' = F_{11}(1 - G_{22}) \left(\frac{2r_s}{\pi^2} \right) \frac{1}{\rho q} - [F_{11}^2(1 - G_{11})(1 - G_{22}) - F_{12}^2(1 - G_{12})^2] \left(\frac{2r_s}{\pi^2} \right)^2 \frac{2}{\rho q^2} \ln \left| \frac{\omega_-}{\omega_+} \right|.$$

Figure 6(b) shows the optical and acoustic plasmon dispersions calculated using the above long-wavelength expressions in an electron–hole double-wire system at $r_s = 1$ in which the plasmon energies are scaled with respect to the hole Fermi energy $E_{Fh} = \rho E_F$. The RPA and STLS approximation results are plotted as the dashed and solid lines, respectively. It is interesting to note that the acoustic plasmon is affected more by the local-field effects than the optical plasmon.

In this work we have mainly considered equal-density double-wire systems. Experimentally, attaining exactly the same density in each wire in realistic systems may be difficult. Our method can easily be generalized to include such cases. It is expected that the collective modes of an unequal-density system will have qualitatively different properties from the modes in identical wires. The semiconducting quantum wires realized so far and used in the experiments are typically characterized by densities of $r_s \sim 1$. It is, however, conceivable that structures having lower densities can be manufactured with advances in growth technology [31]. The many-body effects discussed here would then be more readily applicable to the experimental realizations. CDW-type instabilities discussed in the context of double-quantum-well structures [23] and also in double quantum wires [21, 22] could be explored. We have not systematically calculated the static response functions $\chi_{\pm}(q, 0)$ (obtained by diagonalizing the response matrix with elements χ_{ij} given in equation (1)) for a wide range of parameters R , d , and r_s , but surmise that interesting features of the CDW instability could be studied using our local-field factors.

4. Summary

In summary, we have studied the ground-state correlations in Q1D electron and electron–hole systems in double-quantum-wire structures interacting via a Coulomb potential in the self-consistent scheme of Singwi *et al* [15]. The local-field corrections describing exchange and correlation effects provide an improvement over the RPA results. The ground-state energy is calculated as a function of carrier density in the wires and wire separation. We found that Q1D electron gas, which occurs in semiconducting quantum wires, shows similar behaviour qualitatively to that found in 2D and 3D cases. The collective modes in double-wire systems, in particular electron–hole wires, exhibit a rich structure which could be probed in Raman-scattering-type experiments. We provided expressions for the long-wavelength limits of the plasmon dispersion in electron–hole double quantum wires which could be useful for such studies. Our results should be qualitatively the same for different models of quantum-wire structures, provided that the asymptotic forms of the Coulomb interaction are compatible in the sense discussed by Fantoni and Tosi [28].

Acknowledgments

This work is partially supported by the Scientific and Technical Research Council of Turkey (TUBITAK) under Grant No TBAG-AY/123. We thank Professor G Senatore and Dr C Bulutay for useful discussions, and acknowledge a helpful communication with Professor D Neilson.

References

- [1] Hansen W, Horst M, Kotthaus J P, Merkt U, Sikorski C and Ploog K 1987 *Phys. Rev. Lett.* **58** 2586
Demel T, Heitmann D, Grambow P and Ploog K 1988 *Phys. Rev. B* **38** 12 732
- [2] Goñi A R, Pinczuk A, Weiner J S, Calleja J M, Dennis B S, Pfeiffer L N and West K W 1991 *Phys. Rev. Lett.* **67** 3298
Schmeller A, Goñi A R, Pinczuk A, Reiner J S, Calleja J M, Dennis B S, Pfeiffer L N and West K W 1994 *Phys. Rev. B* **49** 14 778
- [3] Hu G Y and O'Connell R F 1990 *Phys. Rev. B* **42** 1290
- [4] Li Q P and Das Sarma S 1991 *Phys. Rev. B* **43** 11 768
- [5] Hu B Y-K and Das Sarma S 1992 *Phys. Rev. Lett.* **68** 1750
Hu B Y-K and Das Sarma S 1993 *Phys. Rev. B* **48** 5469
See also
Das Sarma S and Hwang E H 1996 *Phys. Rev. B* **54** 1936
- [6] Gold A and Ghazali A 1990 *Phys. Rev. B* **41** 7626
- [7] Sun Y and Kirczenow G 1995 *Can. J. Phys.* **73** 357
- [8] Gold A 1992 *Z. Phys.* **B 89** 213
- [9] Yu J-X and Xia J-B 1996 *Solid State Commun.* **98** 227
- [10] Sólyom J 1979 *Adv. Phys.* **28** 201
For a fairly recent review, see e.g.,
Mattis D C (ed) 1993 *The Many-Body Problem* (Singapore: World Scientific)
- [11] See the calculations by Das Sarma and co-workers [5] for a detailed account of a Fermi-liquid and Luttinger-liquid comparison.
- [12] Friesen W I and Bergersen B 1980 *J. Phys. C: Solid State Phys.* **13** 6627
- [13] Campos V B, Degani M H and Hipólito O 1995 *Superlatt. Microstruct.* **17** 85
Borges A N, Degani M H and Hipólito O 1993 *Superlatt. Microstruct.* **13** 375
- [14] Calmels L and Gold A 1995 *Phys. Rev. B* **51** 8426
- [15] Singwi K S, Tosi M P, Land R H and Sjölander A 1968 *Phys. Rev.* **179** 589
Singwi K S and Tosi M P 1981 *Solid State Physics* vol 36 (New York: Academic) p 177
- [16] Knorr W and Godby R W 1994 *Phys. Rev. B* **50** 1779
- [17] Wu Z and Ruden P P 1993 *J. Appl. Phys.* **74** 6234 and references therein
- [18] Zheng L and MacDonald A H 1994 *Phys. Rev. B* **49** 5522
- [19] Liu L, Świerkowski L, Neilson D and Szymański J 1996 *Phys. Rev. B* **53** 7923
Szymański J, Świerkowski L and Neilson D 1994 *Phys. Rev. B* **50** 11 002
- [20] Zhang C and Tzoar N 1988 *Phys. Rev. B* **38** 5786
See also,
Alatalo M, Pietiläinen P, Chakraborty T and Salmi M A 1994 *Phys. Rev. B* **49** 8277
for a hypernetted-chain integral-equation-based approach.
- [21] Gold A 1992 *Phil. Mag. Lett.* **66** 163
- [22] Wang R and Ruden P P 1995 *Phys. Rev. B* **52** 7826
- [23] Świerkowski L, Neilson D and Szymański J 1991 *Phys. Rev. Lett.* **67** 240
Neilson D, Świerkowski L, Szymański J, and Liu L 1993 *Phys. Rev. Lett.* **71** 4035
- [24] Sjölander A and Stott J 1972 *Phys. Rev. B* **5** 2109
- [25] Williams P F and Bloch A N 1974 *Phys. Rev. B* **10** 1097
- [26] Mermin N D 1970 *Phys. Rev. B* **1** 2362
Das A K 1975 *J. Phys. F: Met. Phys.* **5** 2035
- [27] Pines D and Nozières P 1966 *The Theory of Quantum Liquids* (New York: Benjamin)
Mahan G D 1981 *Many Particle Physics* (New York: Plenum)
- [28] Fantoni R and Tosi M P 1996 *Physica B* **217** 35
- [29] Neilson D, Świerkowski L, Sjölander A and Szymański J 1991 *Phys. Rev. B* **44** 6291
- [30] Vignale G 1988 *Phys. Rev. B* **38** 811
Tanatar B 1994 *Solid State Commun.* **92** 699
- [31] Komori K, Wang X-L, Ogura M, Matsuhata H and Imanishi H 1996 *Appl. Phys. Lett.* **68** 3787